Initial correlations in a nonequilibrium Falicov-Kimball model

Minh-Tien Tran
Asia Pacific Center for Theoretical Physics, POSTECH, Pohang, Gyeongbuk 790-784, Republic of Korea
and Institute of Physics and Electronics, Vietnamese Academy of Science and Technology, 10 Dao Tan, Hanoi 10000, Vietnam
(Received 5 June 2008; published 5 September 2008)

The Keldysh boundary problem in a nonequilibrium Falicov-Kimball model in infinite dimensions is studied within the truncated and self-consistent perturbation theories and the dynamical mean-field theory. Within the model the system is started in equilibrium, and later a uniform electric field is turned on. The Kadanoff-Baym-Wagner equations for the nonequilibrium Green's functions are derived and numerically solved. The contributions of initial correlations are studied by monitoring the system evolution. It is found that the initial correlations are essential for establishing the full electron correlations of the system and are independent of the starting time of preparing the system in equilibrium. By examining the contributions of the initial correlations to the electric current and the double occupation, we find that the contributions are small in relation to the total value of those physical quantities when the interaction is weak, and significantly increase when the interaction is strong. The neglect of initial correlations may cause artifacts in the nonequilibrium properties of the system, especially in the strong-interaction case.

DOI: 10.1103/PhysRevB.78.125103 PACS number(s): 71.27.+a, 71.10.Fd, 05.70.Ln, 05.30.−d

I. INTRODUCTION

The theoretical description of the physical properties of nonequilibrium correlated electron systems is an important problem in condensed-matter physics. Often in transport processes correlated electron systems are driven out of equilibrium by switching on external fields. The systems can be also driven out of equilibrium by suddenly changing their parameters. Nonequilibrium correlated electron systems, which can be realized in many experiments, may have unusual and interesting properties. One such system is the quantum dot attached to two leads through two tunnel junctions.[1–3] The conductance of the dot reveals a nonequilibrium Kondo effect. Other examples are the effects of electron correlations on the nonlinear current-voltage characteristics.[4,5] Recently, experiments with ultracold atomic gases have made it possible to prepare an initial state with a rapid change in system parameters, and observed remarkable subsequent dynamics as a collapse and revival of the initial phase.[6,7]

The many-body formalism for nonequilibrium systems was developed by many people, including Kubo,[8] Schwinger,[9] Kadanoff and Baym,[10] and Keldysh[11] (see also Refs. 12 and 13 for reviews). In particular, Kadanoff and Baym[10] constructed a system of equations for the nonequilibrium Green's functions. Parallel to this development, Keldysh[11] also derived a perturbation theory for the nonequilibrium Green's functions. Like the Feynman perturbation theory for equilibrium systems,[14] the Keldysh nonequilibrium perturbation theory is based on the assumption of an adiabatic switching on of the many-body interactions. The assumption is necessary for the application of the Wick theorem, which requires a quadratic form of the system Hamiltonian at the initial preparation of the system. While the assumption is exactly proved in scattering theory,[14] its application to nonequilibrium many-body systems imposes restrictions.[15–17] It turns out that the assumption corresponds to the neglect of the so-called initial correlations.[15–17] Despite the neglect of the initial correlations, the Keldysh theory is widely used in the study of nonequilibrium systems. Wagner[17] unified the Feynman, Matsubara, and Keldysh perturbation theories into a single many-body formalism in which neither a special form of the Hamiltonian at the initial time nor the subsequent time development of the system is restricted. He introduced a matrix representation for the contour-ordered Green's function and derived the Kadanoff-Baym equations for the nonequilibrium Green's functions. In the Kadanoff-Baym-Wagner formalism, the initial correlations are fully taken into account. While the nonequilibrium formalism is well established, the role of the initial correlations is less attended, especially for nonequilibrium strongly correlated electron systems. In particular, it would be desirable to test whether the initial correlations which are neglected in the Keldysh formalism are negligible or not. The difficulties of studying the initial correlations are mostly due to the lack of methods for getting the exact solutions of nonequilibrium correlated electron systems.

In the last decade, the dynamical mean-field theory (DMFT) was developed.[18,19] In the equilibrium case the theory is widely and successfully applied to the study of strongly correlated electron systems. The DMFT gives the exact solutions in infinite dimensions. Recently, a version of the DMFT for nonequilibrium systems was developed.[20] The nonequilibrium dynamical mean-field theory (NEDMFT) is formally formulated on the same basis as that of the equilibrium DMFT. Like the equilibrium case, in infinite dimensions the self-energy of nonequilibrium systems becomes a local function in space. As a consequence, it can be self-consistently determined by mapping the lattice problem onto an effective problem of a single site embedded in a self-consistent effective medium. When the self-consistent equations are solved, the nonequilibrium Green's functions are obtained and various physical quantities can be calculated.

The aim of the present paper is twofold. First, we study the contributions of the initial correlations in a nonequilibrium correlated electron system. The initial correlations are studied within truncated and self-consistent perturbation theories as well as within the NEDMFT. The Keldysh per-

turbation theory usually argues for the neglect of the initial correlations. However, in the present paper the results obtained within the truncated and self-consistent perturbation theories show that the initial correlations are always finite even when the initial time is in the remote past limit. In the infinite dimension limit, the initial correlations can also be obtained exactly since in this limit the NEDMFT gives the exact solutions. In such way one can find under what circumstance the Keldysh formalism is safely applied to nonequilibrium correlated electron systems. The second aim of the present paper is to derive the Kadanoff-Baym-Wagner equations for the nonequilibrium Green's functions within the NEDMFT. These equations are an alternative to the original NEDMFT equations for the contour-ordered Green's function.[20] Within the Kadanoff-Baym-Wagner formalism, the nonequilibrium Green's functions clearly satisfy their boundary conditions. The Kadanoff-Baym-Wagner formalism already includes the Keldysh formalism as its part, and it is suitable for studying the initial correlations. In this paper we will examine the initial correlations within a Keldysh boundary problem. The problem works in a system which is first started in equilibrium and then is driven out of equilibrium by turning on of an external field. The model which we adopt to describe the system is a nonequilibrium Falicov-Kimball model. The Falicov-Kimball model (FKM) was first introduced for modeling a metal-insulator transition at equilibrium.[21] The model is one of the simplest models for studying strongly correlated electron systems. The FKM describes conduction electrons interacting via a repulsive contact potential with localized electrons. It can be viewed as a simplified Hubbard model where electrons with down spin are frozen and do not hop. Much progress has been made on solving this model in both exact and approximation ways, where all the properties of the conduction electrons at equilibrium are well known.[22–24] At equilibrium the FKM describes a metal-insulator transition for the homogeneous phase.[22–24] The Coulomb interaction is divided into two ranges: the weak-interaction range, where the interaction strength is smaller than the half bare bandwidth, and the strong-interaction one, the opposite case. For weak interactions the system is metallic, and for strong ones the system is an insulator. The system is driven out of equilibrium by a constant electric field. The electric field is switched on at some time after the initial preparation of the system in equilibrium. This nonequilibrium FKM was introduced by Freericks *et al.*[20] in the study of the Bloch oscillations in the electric current within the NEDMFT. In the present paper we derive the Kadanoff-Baym-Wagner equations of the NEDMFT for the nonequilibrium FKM, and calculate the contributions of the initial correlations to the electric current and the double occupation. It is found that the contributions of the initial correlations to the electric current and the double occupation are small in relation to the full value of those physical quantities in the weak-interaction case, and significantly increases in the strong-interaction case. However, without the initial correlations the system cannot restore full electron correlations even before the turning on of the electric field. The neglect of the initial correlations may cause artifacts in the nonequilibrium properties of the system.

The paper is organized as follows: In Sec. II we present the Kadanoff-Baym-Wagner nonequilibrium formalism, and describe the nonequilibrium FKM. In Secs. III–V we present the studies of the model within the truncated and self-consistent perturbation theories and the NEDMFT. Section VI is the conclusion.

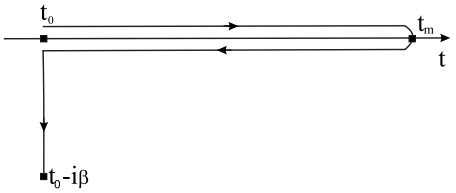

FIG. 1. Kadanoff-Baym contour for the two-time Green's functions in nonequilibrium.

II. FORMALISM AND MODEL

We consider the Keldysh boundary problem in a nonequilibrium system which is first prepared in equilibrium and then is driven out of equilibrium by switching on of an external field or by a sudden change of its parameters. Specifically, at an initial time t_0 the system is prepared in equilibrium, which is defined by the equilibrium Hamiltonian H_{eq} and temperature $1/\beta$. At time $t=0$ ($t_0<0$) an external field is switched on or its parameters are suddenly changed. Usually, in nonequilibrium systems the time translational invariance is not valid, and Green's functions, which are employed in studying the physical properties of the systems, depend on the two time variables. The nonequilibrium formalism works with the so-called contour-ordered Green's function, which is defined for the time variables on the Kadanoff-Baym contour.[10–13] The Kadanoff-Baym contour is shown in Fig. 1. The contour starts at the initial time t_0, runs out up to maximal time t_m, then returns to the initial time, and finally moves parallel to the negative imaginary axis a distance β. At the initial time t_0, the system is always in equilibrium. The Kadanoff-Baym contour is suitable for deriving the Dyson equation for the contour-ordered Green's function. Keldysh[11] also introduced a similar contour for the contour-ordered Green's function. The Keldysh contour is basically the same as the Kadanoff-Baym contour, but it neglects the last contour branch parallel to the imaginary axis and limits t_0 to minus infinity. The neglect of the last branch of the contour corresponds to the neglect of initial correlations. The contour-ordered Green's function is defined by

$$G^c(i,j|\bar{t},\bar{t}') = -i\langle \mathcal{T}_c c_i(\bar{t}) c_j^\dagger(\bar{t}')\rangle = -i\theta^c(\bar{t},\bar{t}')\langle c_i(\bar{t}) c_j^\dagger(\bar{t}')\rangle + i\theta^c(\bar{t}',\bar{t})\langle c_j^\dagger(\bar{t}') c_i(\bar{t})\rangle, \quad (1)$$

where $c_i^\dagger$ (c_i) are the creation (annihilation) operators for electrons at site i. The time evolution of the operators on the Kadanoff-Baym contour is defined in the Heisenberg picture. $\mathcal{T}_c$ is the time ordering on the Kadanoff-Baym contour and it is defined via the contour step function $\theta^c(\bar{t},\bar{t}')$. $\theta^c(\bar{t},\bar{t}')$ is equal to 1 if $\bar{t}$ lies after $\bar{t}'$ on the contour, and it is equal to 0 if otherwise. The averages in Eq. (1) are the statistical averages over the equilibrium Hamiltonian H_{eq} at temperature $1/\beta$. The Kadanoff-Baym contour consists of three time branches: The first branch is chronological, the second one is

antichronological, and the last one is parallel to the imaginary axis. Thus, we can represent the contour-ordered Green's function by a 3×3 matrix $G^{\alpha\gamma}(\bar{t},\bar{t}')$, where $\bar{t}$ locates on the αth branch and $\bar{t}'$ locates on the γth branch. In such way, the contour-ordered Green's function has nine component Green's functions; however they are not independent. Wagner[17] reduced the matrix representation of the contour-ordered Green's function to a matrix form of six component Green's functions, and five of them are independent. The Wagner matrix representation for the contour-ordered Green's function can be written as follows:[17]

$$\hat{G}=\begin{pmatrix} G^R & G^K & \sqrt{2}G^{\rceil} \\ 0 & G^A & 0 \\ 0 & \sqrt{2}G^{\lceil} & G^M \end{pmatrix}, \tag{2}$$

where

$$G^R(t,t')=G^{11}(t,t')-G^{12}(t,t')=-i\theta(t-t')\langle\{c_i(t),c_j^\dagger(t')\}\rangle,$$

$$G^A(t,t')=G^{12}(t,t')-G^{22}(t,t')=i\theta(t'-t)\langle\{c_i(t),c_j^\dagger(t')\}\rangle,$$

$$G^K(t,t')=G^{12}(t,t')+G^{21}(t,t')=-i\langle[c_i(t),c_j^\dagger(t')]\rangle,$$

$$G^M(\tau,\tau')=G^{33}(t_0-i\tau,t_0-i\tau')=-i\langle\mathcal{T}_\tau c_i(t_0-i\tau)c_j^\dagger(t_0-i\tau')\rangle,$$

$$G^{\rceil}(t,\tau')=G^{13}(t,t_0-i\tau')=i\langle c_j^\dagger(t_0-i\tau')c_i(t)\rangle,$$

$$G^{\lceil}(\tau,t')=G^{31}(t_0-i\tau,t')=-i\langle c_i(t_0-i\tau)c_j^\dagger(t')\rangle,$$

where t and t' are real times and $0\le\tau,\tau'\le\beta$. In the above equations we have used the commutator symbol $[A,B]=AB-BA$ and the anticommutator symbol $\{A,B\}=AB+BA$. $G^{R(A)}$ are the retarded (advanced) Green's functions, and G^K is the Keldysh Green's function. These Green's functions are defined totally on the real time axis. G^M is the Matsubara Green's function and is defined on the imaginary time branch of the Kadanoff-Baym contour. Note that the above definition of the Matsubara Green's function differs from the standard one by a factor of i.[14] The Green's functions $G^{\rceil}$ and $G^{\lceil}$ have one time variable on the real time axis, and the other variable is on the imaginary time branch.[25] They do not have a specific name; however we will refer to them as the right and left time mixing Green's functions, respectively. The left corner 2×2 matrix in the Wagner matrix representation in Eq. (2) is the Keldysh representation of the nonequilibrium Green's functions in the Keldysh perturbation theory.[11] The Matsubara Green's function is just the equilibrium Green's function at temperature $1/\beta$. It couples with the Keldysh Green's function through the time mixing Green's functions. If the time mixing Green's functions are neglected, the Kadanoff-Baym-Wagner formalism reduces to the Keldysh formalism.

Within the Wagner matrix representation, the Dyson equation for the nonequilibrium Green's functions can be written in the standard form like that in the equilibrium case,

$$\hat{G}=\hat{G}_0+\hat{G}_0\bullet\hat{\Sigma}\bullet\hat{G}, \tag{3}$$

where $\hat{G}_0$ is the bare Green's function and $\hat{\Sigma}$ is the self-energy. The self-energy is also written in the Wagner matrix representation,

$$\hat{\Sigma}=\begin{pmatrix} \Sigma^R & \Sigma^K & \sqrt{2}\Sigma^{\rceil} \\ 0 & \Sigma^A & 0 \\ 0 & \sqrt{2}\Sigma^{\lceil} & \Sigma^M \end{pmatrix}. \tag{4}$$

Note that in Dyson equation (3), the product symbol $\bullet$ denotes not only the matrix multiplication but also the integration over the time variables. We also omitted other variable notations such as those of momentum or spin to simplify the equation writing. We introduce the inverse matrix Green's function $\hat{\tilde{G}}$ by using the standard definition

$$\hat{\tilde{G}}\bullet\hat{G}=\hat{1}. \tag{5}$$

The inverse matrix Green's function is also presented in the Wagner matrix representation. One can find its elements by explicitly writing the component equations of Eq. (5):

$$\tilde{G}^{R/A}\cdot G^{R/A}=\hat{1}, \tag{6}$$

$$\tilde{G}^M\star G^M=\hat{1}, \tag{7}$$

$$\tilde{G}^R\cdot G^K+\tilde{G}^K\cdot G^A+2\tilde{G}^{\rceil}\star G^{\lceil}=0, \tag{8}$$

$$\tilde{G}^R\cdot G^{\rceil}+\tilde{G}^{\rceil}\star G^M=0, \tag{9}$$

$$\tilde{G}^{\lceil}\cdot G^A+\tilde{G}^M\star G^{\lceil}=0. \tag{10}$$

Here the dot and star products are the integrations over the real time and the imaginary time variables, respectively, i.e.,

$$(A\cdot B)(\bar{t},\bar{t}')=\int_{t_0}^{t_m}dt_1A(\bar{t},t_1)B(t_1,\bar{t}'),$$

$$(A\star B)(\bar{t},\bar{t}')=-i\int_0^\beta d\tau_1A(\bar{t},\tau_1)B(\tau_1,\bar{t}').$$

The symbol $\hat{1}$ is just the delta function of the time variables. For real time variables it is $\delta(t-t')$, and for imaginary time variables it is $i\delta(\tau-\tau')$. One can view $\tilde{G}^{R/A/M}$ as the inverse matrices of $G^{R/A/M}$ in continuous time variables. However, $\tilde{G}^{K/\rceil/\lceil}$ are not inverses of the corresponding Green's functions. Dyson equation (3) can be rewritten as follows:

$$\hat{\tilde{G}}_0\bullet\hat{G}=\hat{1}+\hat{\tilde{\Sigma}}\bullet\hat{G}, \tag{11}$$

where $\hat{\tilde{G}}_0$ is the inverse matrix of $\hat{G}_0$, and its elements can be found from Eqs. (6)–(10) for the bare Green's functions. Equation (11) can be written in the explicit form for the component Green's functions:

$$\tilde{G}_0^{R/A}\cdot G^{R/A}=\hat{1}+\Sigma^{R/A}\cdot G^{R/A}, \tag{12}$$

$$\tilde{G}_0^M \star G^M = \hat{1} + \Sigma^M \star G^M, \tag{13}$$

$$\tilde{G}_0^R \cdot G^\rceil = \Sigma^R \cdot G^\rceil + (\Sigma^\rceil - \tilde{G}_0^\rceil) \star G^M, \tag{14}$$

$$\tilde{G}_0^M \star G^\lceil = \Sigma^M \star G^\lceil + (\Sigma^\lceil - \tilde{G}_0^\lceil) \cdot G^A, \tag{15}$$

$$\tilde{G}_0^R \cdot G^K = \Sigma^R \cdot G^K + (\Sigma^K - \tilde{G}_0^K) \cdot G^A + 2(\Sigma^\rceil - \tilde{G}_0^\rceil) \star G^\lceil. \tag{16}$$

Equations (12)–(16) are just the Kadanoff-Baym equations for the nonequilibrium Green's functions written in the Wagner representation. In the standard Kadanoff-Baym equations,[10,17] the inverse bare Green's functions are written in the form of differential operators. These differential equations also require additional boundary conditions. In Kadanoff-Baym-Wagner equations (12)–(16), the inverse bare Green's functions have their explicit forms and they satisfy their boundary conditions. Instead of differential-integral equations in the Kadanoff-Baym formalism of the contour-ordered Green's function, Kadanoff-Baym-Wagner equations (12)–(16) are just integral equations. Once the self-energy is computable, Kadanoff-Baym-Wagner equations (12)–(16) can be solved. First we solve Eqs. (12) and (13) for the retarded, advanced, and Matsubara Green's functions. These equations can be solved independently. Certainly, the advanced Green's function can be quickly obtained from the retarded Green's function by using the relation

$$G^A(t,t') = [G^R(t',t)]^*. \tag{17}$$

Moreover, Matsubara equation (13) is the equilibrium equation and we can also use the equilibrium techniques to calculate the Matsubara Green's function. Next we use the retarded, advanced, and Matsubara Green's functions as the inputs and solve the next two equations for the time mixing Green's functions. Finally, we solve the last equation for the Keldysh Green's function. The Kadanoff-Baym-Wagner equation for Keldysh Green's function (16) can be rewritten as

$$\begin{aligned} G^K = {} & (\hat{1} + G^R \cdot \Sigma^R) \cdot G_0^K \cdot (\hat{1} + \Sigma^A \cdot G^A) + G^R \cdot \Sigma^K \cdot G^A \\ & - 2G^R \cdot [\tilde{G}_0^\rceil \star G_0^M \star \tilde{G}_0^\lceil - (\Sigma^\rceil - \tilde{G}_0^\rceil) \\ & \star G^M \star (\Sigma^\lceil - \tilde{G}_0^\lceil)] \cdot G^A. \end{aligned} \tag{18}$$

Here we have used Eqs. (8) and (10) for $\tilde{G}_0^K$ and $\tilde{G}_0^\lceil$ and Eqs. (12) and (15) for the retarded (advanced) and time mixing Green's functions. If the time mixing Green's functions are neglected, Kadanoff-Baym-Wagner equation (18) is reduced to the Keldysh equation

$$G^K = (\hat{1} + G^R \cdot \Sigma^R) \cdot G_0^K \cdot (\hat{1} + \Sigma^A \cdot G^A) + G^R \cdot \Sigma^K \cdot G^A. \tag{19}$$

The Keldysh formalism neglects the contributions generated from the dynamics of the system in the imaginary time branch of the Kadanoff-Baym contour. Since at the initial time t_0 the system is prepared in equilibrium with full interaction, the neglected contributions are correlations of electrons between the initial time and an advanced time. Indeed, if we neglect the correlation effects of the Matsubara and the time mixing Green's functions (i.e., $\Sigma^{M/\rceil}=0$), the last term in Eq. (18) vanishes, and we again obtain the Keldysh equation. The neglected contributions are called initial correlations.[13,15–17] The initial correlations distinguish between the Kadanoff-Baym-Wagner and the Keldysh formalisms. One can notice that the equations for the retarded and advanced Green's functions are decoupled from the system of equations. Hence the nonequilibrium density of states remains the same in both the Kadanoff-Baym-Wagner and the Keldysh formalisms. The initial correlations do not affect the nonequilibrium density of states. They affect only the nonequilibrium distribution function. Thus the initial correlations give contributions only to physical quantities which depend on the nonequilibrium distribution function.

The model we will study is the FKM with the external electric field turned on at $t=0$. At the initial time t_0, the system is prepared in equilibrium with temperature $1/\beta$ and the FKM Hamiltonian

$$H_{\mathrm{eq}} = -\sum_{i,j} J_{ij} c_i^\dagger c_j - \mu \sum_i c_i^\dagger c_i + E_f \sum_i f_i^\dagger f_i + U \sum_i c_i^\dagger c_i f_i^\dagger f_i, \tag{20}$$

where $c_i^\dagger$ (c_i) are the creation (annihilation) operators for conduction electrons at site i, and $f_i^\dagger$ (f_i) are the creation (annihilation) operators for localized electrons at site i. J_{ij} is the hopping matrix of conduction electrons; it is equal to J for nearest-neighbor sites, and it is 0 otherwise. U is the strength of the interaction between the conduction and localized electrons. μ and E_f are the chemical potentials of the conduction and localized electrons, respectively. In this paper we will only consider the half filling case. It turns out that in the half filling case, $\mu=-E_f=U/2$. At time $t=0$ a spatially uniform electric field is turned on. We choose the gauge with vanishing of the scalar potential for the electric field. As a result the electric field is described by a spatially uniform vector potential $\mathbf{A}(t)=-\theta(t)\mathbf{E}t$. The electric field couples to the conduction electrons through the Peierls substitution for the hopping matrix,

$$\begin{aligned} J_{ij} \to J_{ij} \exp\left[-ie \int_{\mathbf{R}_i}^{\mathbf{R}_j} d\mathbf{r} \mathbf{A}(\mathbf{r},t) \right] \\ = J_{ij} \exp[-ie\mathbf{A}(t)(\mathbf{R}_j - \mathbf{R}_i)]. \end{aligned} \tag{21}$$

By replacing the hopping matrix in Hamiltonian in Eq. (20) with Eq. (21), we obtain the full nonequilibrium Hamiltonian of the system. This nonequilibrium FKM was introduced by Freericks *et al.*[20] in the study of the NEDMFT. The considered nonequilibrium FKM differs from the equilibrium FKM only by the bare energy spectra

$$\varepsilon(\mathbf{k},t) = \varepsilon(\mathbf{k} - e\mathbf{A}(t)) = -2J \sum_{i=1}^{d} \cos[k_i - eA_i(t)], \tag{22}$$

where d is the space dimension of the system. We will consider the case where the electric field lies along the elementary cell diagonal,

$$\mathbf{A}(t) = A(t)(1, 1, \ldots, 1).$$

In this case the bare energy spectra becomes

$$\varepsilon(\mathbf{k}, t) = \cos[eA(t)]\varepsilon(\mathbf{k}) + \sin[eA(t)]\bar{\varepsilon}(\mathbf{k}), \tag{23}$$

where

$$\varepsilon(\mathbf{k}) = -2J\sum_{i=1}^{d}\cos(k_i),$$

$$\bar{\varepsilon}(\mathbf{k}) = -2J\sum_{i=1}^{d}\sin(k_i).$$

In the limit of infinite dimensions, $d \to \infty$, the bare density of states has a double Gaussian form,

$$\rho(\varepsilon, \bar{\varepsilon}) = \rho_0(\varepsilon)\rho_0(\bar{\varepsilon}), \tag{24}$$

where $\rho_0(\varepsilon) = \exp(-\varepsilon^2)/\sqrt{\pi}$. Here we have used $J^* = J\sqrt{d}$ as the unit of energy.

The nonequilibrium bare Green's functions can be found from the equations of motion. The equation of motion for the retarded Green's function reads

$$[i\partial_t + \mu_0 - \varepsilon(\mathbf{k}, t)]G_0^R(\mathbf{k}|t, t') = \delta(t - t'),$$

where μ_0 is the chemical potential of the noninteracting conduction electrons. At half filling, $\mu_0 = 0$. With the boundary condition $G_0^R(\mathbf{k}|t, t) = -i$, we can find the bare nonequilibrium retarded Green's function

$$G_0^R(\mathbf{k}|t, t') = -i\theta(t - t')e^{i\mu_0(t-t')}\exp\left[-i\int_{t'}^{t} dt_1 \varepsilon(\mathbf{k}, t_1)\right]. \tag{25}$$

Similarly, one can find the bare advanced, Keldysh, and Matsubara Green's functions

$$G_0^A(\mathbf{k}|t, t') = i\theta(t' - t)e^{i\mu_0(t-t')}\exp\left[-i\int_{t'}^{t} dt_1 \varepsilon(\mathbf{k}, t_1)\right], \tag{26}$$

$$G_0^K(\mathbf{k}|t, t') = i[2f(\varepsilon(\mathbf{k}) - \mu_0) - 1]e^{i\mu_0(t-t')} \times \exp\left[-i\int_{t'}^{t} dt_1 \varepsilon(\mathbf{k}, t_1)\right], \tag{27}$$

$$G_0^M(\mathbf{k}|\tau, \tau') = -i[\theta(\tau - \tau') - f(\varepsilon(\mathbf{k}) - \mu_0)]e^{-[\varepsilon(\mathbf{k})-\mu_0](\tau-\tau')}, \tag{28}$$

where $f(\varepsilon) = 1/[\exp(\beta\varepsilon) + 1]$ is the Fermi-Dirac distribution function. The bare right time mixing Green's function can be found from the equation of motion

$$[i\partial_t + \mu_0 - \varepsilon(\mathbf{k}, t)]G_0^{\rceil}(\mathbf{k}|t, \tau') = 0,$$

with the boundary condition $G_0^{\rceil}(\mathbf{k}|t_0, \tau') = G_0^M(0, \tau')$. We obtain

$$\begin{aligned} G_0^{\rceil}(\mathbf{k}|t, \tau') &= -i[\theta(-\tau') - f(\varepsilon(\mathbf{k}) - \mu_0)] \\ &\times e^{[\varepsilon(\mathbf{k})-\mu_0]\tau'}e^{i\mu_0(t-t_0)}\exp\left[-i\int_{t_0}^{t} dt_1 \varepsilon(\mathbf{k}, t_1)\right] \\ &= iG_0^R(\mathbf{k}|t, t_0)G_0^M(\mathbf{k}|0, \tau'), \end{aligned} \tag{29}$$

since $t \geq t_0$. Similarly, the bare left time mixing Green's function is

$$\begin{aligned} G_0^{\lceil}(\mathbf{k}|\tau, t') &= -i[\theta(\tau) - f(\varepsilon(\mathbf{k}) - \mu_0)] \\ &\times e^{-[\varepsilon(\mathbf{k})-\mu_0]\tau}e^{i\mu_0(t'-t_0)}\exp\left[i\int_{t_0}^{t'} dt_1 \varepsilon(\mathbf{k}, t_1)\right] \\ &= -iG_0^M(\mathbf{k}|\tau, 0)G_0^A(\mathbf{k}|t_0, t'). \end{aligned} \tag{30}$$

The nonequilibrium bare Green's functions clearly satisfy their boundary conditions. When the self-energy is computable, it, together with the bare Green's functions, fully determines the nonequilibrium Green's functions via Kadanoff-Baym-Wagner equations (12)–(16). In Secs. III–V we will solve the Kadanoff-Baym-Wagner equations with the self-energy calculated within the truncated and self-consistent perturbation theories as well as within the NEDMFT.

III. TRUNCATED PERTURBATION THEORY

In this section we calculate the nonequilibrium Green's functions and the electric current within the truncated perturbation theory of second order in U. The perturbation calculations were previously performed within the Keldysh nonequilibrium perturbation theory,[26] where the initial correlations are neglected. The purpose of this section is to find the contributions of the initial correlations to the electric current within the truncated perturbation theory.

In the half filling case, the first-order perturbation contributions to the self-energy vanish.[26] The second-order self-energy can be found by expanding the contour-ordered Green's function to second order in U. One can find[26]

$$\Sigma_2^{\alpha}(t, t') = U^2 n_f(1 - n_f)\frac{1}{N}\sum_{\mathbf{k}} G_0^{\alpha}(\mathbf{k}|t, t'), \tag{31}$$

where $\alpha = R, A, M, K, \rceil, \lceil$ and $n_f = 1/2$ is the density of the localized electrons at half filling. Within the second-order perturbation, the self-energy does not depend on momentum. This feature is similar to the DMFT, where the self-energy is a function of time variables only. Using Dyson equation (3), we can obtain the nonequilibrium Green's functions up to second order in U,

$$G_2^{\alpha}(\mathbf{k}|t, t') = G_0^{\alpha}(\mathbf{k}|t, t') + \Delta G_2^{\alpha}(\mathbf{k}|t, t'), \tag{32}$$

where

$$\Delta G_2^{R/A} = G_0^{R/A} \cdot \Sigma_2^{R/A} \cdot G_0^{R/A}, \tag{33}$$

$$\Delta G_2^{M} = G_0^{M} \star \Sigma_2^{M} \star G_0^{M}, \tag{34}$$

$$\Delta G_2^{\lceil} = G_0^{\lceil} \cdot \Sigma_2^{A} \cdot G_0^{A} + G_0^{M} \star \Sigma_2^{\lceil} \cdot G_0^{A} + G_0^{M} \star \Sigma_2^{M} \star G_0^{\lceil}, \tag{35}$$

$$\Delta G_2^{\rceil} = G_0^R \cdot \Sigma_2^R \cdot G_0^{\rceil} + G_0^R \cdot \Sigma_2^{\rceil} \star G_0^M + G_0^{\rceil} \star \Sigma_2^M \star G_0^M, \tag{36}$$

$$\Delta G_2^K = G_0^R \cdot \Sigma_2^R \cdot G_0^K + G_0^R \cdot \Sigma_2^K \cdot G_0^A + G_0^K \cdot \Sigma_2^A \cdot G_0^A + 2G_0^R \cdot \Sigma_2^{\rceil} \star G_0^{\lceil} + 2G_0^{\rceil} \star \Sigma_2^{\lceil} \cdot G_0^A + 2G_0^{\rceil} \star \Sigma_2^M \star G_0^{\lceil}. \tag{37}$$

Here, for simplicity we omitted the variable notations in the Green's functions and the self-energy. In comparison to the Keldysh perturbation theory, the Kadanoff-Baym-Wagner perturbation expansions of the retarded and advanced Green's functions remain unchanged.[26] However, the second-order perturbation expansion of the Keldysh Green's function is different. It consists of two parts. The first part is the first three terms in Eq. (37), which are also the perturbation contributions within the Keldysh perturbation theory,[26] and the second part is the remaining last three terms, which are additional contributions generated from the initial correlations. The Keldysh perturbation theory neglects the second part.

The electric current can be calculated by evaluating

$$\mathbf{I}(t) = -ie\frac{1}{N}\sum_{\mathbf{k}} \mathbf{v}[\mathbf{k} - e\mathbf{A}(t)]G^<(\mathbf{k}|t,t), \tag{38}$$

where $v_i(\mathbf{k}) = J^* \sin(k_i)/\sqrt{d}$ is the velocity component and $G^<(\mathbf{k}|t,t)$ is the equal time lesser Green's function, which can be calculated from the Keldysh Green's function by using the relation

$$G^<(\mathbf{k}|t,t) = \frac{1}{2}[G^K(\mathbf{k}|t,t) + i]. \tag{39}$$

When the electric field lies along the diagonal, all components of the electric current are equal, and the magnitude of the current is

$$I(t) = \sqrt{d}\mathbf{I}_i(t). \tag{40}$$

By inserting the second-order perturbation expansions of the self-energy in Eq. (31) and of the Green's functions in Eq. (32) into the current formulas in Eqs. (38)–(40), we obtain the electric current up to order U^2,

$$I_2(t) = I_0(t) + \Delta I_2(t), \tag{41}$$

where $I_0(t)$ and $\Delta I_2(t)$ are the zeroth- and second-order contributions to the current. The zeroth-order current is

$$I_0(t) = j_0 \int d\varepsilon \rho_0(\varepsilon)\varepsilon f(\varepsilon)\sin[eA(t)], \tag{42}$$

where $j_0 = e/\sqrt{d}$. It is the electric current in the noninteraction case. It exhibits the Bloch oscillations with period $2\pi/E$, and its amplitude is independent of time. In the noninteraction case, the Bloch oscillations of the current occur when the noninteracting electrons move in a lattice under a constant electric field. In this case the system is a perfect conductor; the periodicity of the lattice restricts the wave vector to lie in the first Brillouin zone that leads to the oscillations of the current.

After some analytical calculations, we also obtain the second-order perturbation contributions to the current strictly in the half filling case,

$$\Delta I_2(t) = \Delta I_2^K(t) + \Delta I_2^{\mathrm{ic}}(t), \tag{43}$$

$$\begin{aligned}\Delta I_2^K(t) = {} & j_0 \frac{U^2}{4}\int_{t_0}^{t} dt_1 \int_{t_0}^{t_1} dt_2 \int d\varepsilon \rho(\varepsilon)\tanh\left(\frac{\beta\varepsilon}{2}\right) \\ & \times \exp\left[-\frac{1}{4}C^2(t_2,t_1) - \frac{1}{2}S^2(t_2,t_1)\right]\left\{\varepsilon \cos[\varepsilon C(t_2,t_1)]\sin[eA(t)] + \frac{1}{2}\sin[\varepsilon C(t2,t1)]S(t_2,t_1)\cos[eA(t)]\right\} \\ & + j_0 \frac{U^2}{16}\int_{t_0}^{t} dt_1 \int_{t_0}^{t} dt_2 \int d\varepsilon \rho(\varepsilon)\tanh\left(\frac{\beta\varepsilon}{2}\right)\exp\left[-\frac{1}{4}C^2(t_2,t_1) - \frac{1}{2}S^2(t_2,t_1)\right]\sin[\varepsilon C(t_2,t_1)]\{C(t_2,t_1)\sin[eA(t)] \\ & - S(t_2,t_1)\cos[eA(t)]\},\end{aligned} \tag{44}$$

$$\begin{aligned}\Delta I_2^{\mathrm{ic}}(t) = {} & j_0 \frac{U^2}{4}\int_{t_0}^{t} dt_1 \int d\varepsilon \int d\varepsilon' \rho(\varepsilon)\rho(\varepsilon')\exp\left[-\frac{1}{2}S^2(t_1,t_0) + i(\varepsilon - \varepsilon')C(t_1,t_0)\right]\frac{f(\varepsilon) - f(\varepsilon')}{\varepsilon' - \varepsilon} \\ & \times \{S(t_1,t_0)\cos[eA(t)] + i(\varepsilon - \varepsilon')\sin[eA(t)]\} + j_0 \frac{U^2}{4}\int d\varepsilon \int d\varepsilon' \rho(\varepsilon)\rho(\varepsilon')f(\varepsilon)f(-\varepsilon)\varepsilon \sin[eA(t)] \\ & \times \left[\frac{e^{\beta(\varepsilon-\varepsilon')} - \beta(\varepsilon - \varepsilon') - 1}{(\varepsilon - \varepsilon')^2} - f(\varepsilon')\frac{e^{\beta(\varepsilon-\varepsilon')} + e^{-\beta(\varepsilon-\varepsilon')} - 2}{(\varepsilon - \varepsilon')^2}\right].\end{aligned} \tag{45}$$

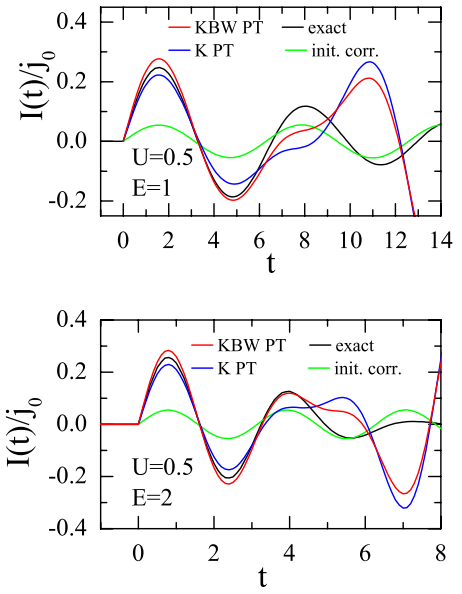

FIG. 2. (Color online) The time dependence of the electric current calculated within the Kadanoff-Baym-Wagner (KBW; red line) and the Keldysh (K; blue line) perturbation theories (PTs). The exact NEDMFT calculation result and the initial correlation contribution to the current are presented as the black and green lines, respectively. The model parameters are $U=0.5$, $\beta=10$, $t_0=-10$, and $E=1$ ($E=2$) for the upper (lower) panel.

Here in order to simplify the expression, we have introduced the functions

$$C(t_2,t_1) = \int_{t1}^{t_2} dt' \cos[eA(t')],$$

$$S(t_2,t_1) = \int_{t1}^{t_2} dt' \sin[eA(t')].$$

Like the Keldysh Green's function, the second-order current also consists of two parts, $\Delta I_2^K(t)$ and $\Delta I_2^{\rm ic}(t)$. The first part, $\Delta I_2^K(t)$, consists of the second-order contributions within the Keldysh perturbation theory.[26] The second part, $\Delta I_2^{\rm ic}(t)$, consists of the contributions of the initial correlations. The second part is beyond the Keldysh perturbation theory.

In Fig. 2 we plot the electric current calculated within the Kadanoff-Baym-Wagner and the Keldysh perturbation theories up to second order in U. For comparison we also plot the exact result which is obtained by performing the NEDMFT calculations (see Sec. V). It shows that the current has the Bloch oscillations with period of $2\pi/E$, like the current in the noninteraction case.[20] However, the amplitude of the current varies with time. The perturbation theories give reasonable results for times smaller than $\sim 2/U$. The Kadanoff-Baym-Wagner perturbation theory overestimates the current, while the Keldysh perturbation theory underestimates it. Figure 2 also shows that the Kadanoff-Baym-Wagner perturbation result is closer to the exact solution than the Keldysh perturbation one at times right before the perturbation theories are broken down. In Fig. 2 we also plot the initial correlation contribution $\Delta I_2^{\rm ic}(t)$ to the current. This part of the current also oscillates with the same period as of the full current. In Fig. 3 we plot the initial correlation part of the current for various values of U and E. In contrast to the full current, the amplitude of the initial correlation part does not significantly vary with time. Since the initial correlation contribution is calculated within the second-order perturbation theory, its amplitude is proportional to U^2 and almost independent of the electric field. Usually, the Keldysh perturbation theory argues that the initial correlations vanish when the initial time approaches minus infinity. In Fig. 4 we plot the current and its initial correlation part at a fixed time as functions of the initial time t_0. It shows that both the current and its initial correlation part quickly approach constant values when $|t_0|$ increases. Even for $t_0=-5$, the current and its initial correlation part already reach the constant values. The initial correlations never vanish, even when $t_0 \to -\infty$. Thus the Keldysh perturbation theory always neglects the nonvanishing initial correlations. However, within the truncated perturbation theory, both the Keldysh and the Kadanoff-Baym-Wagner formalisms only qualitatively describe the physical properties when the perturbation theory works. The

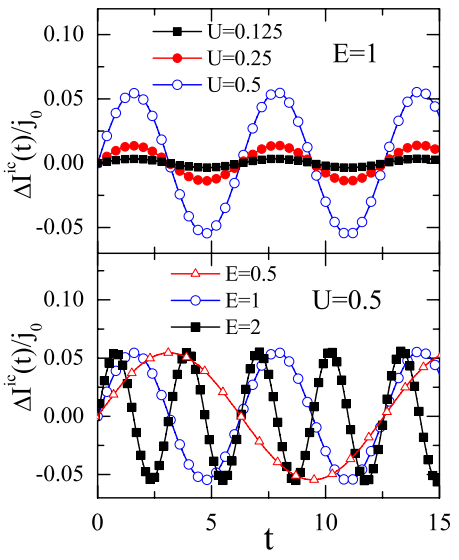

FIG. 3. (Color online)The second-order initial correlation contribution to the current as a function of time for various U and E ($t_0=-10$ and $\beta=10$).

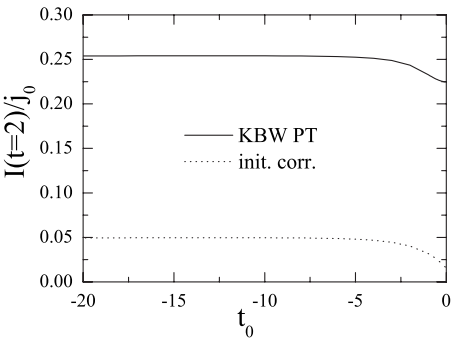

FIG. 4. The electric current (solid line) calculated within the KBW PT and its initial correlation part (dotted line) at time $t=2$ as functions of the initial time t_0 for $U=0.5$, $E=1$, and $\beta=10$.

initial correlations do not qualitatively change the perturbation results. Thus, the use of the Keldysh perturbation theory is still convenient in the nonequilibrium study due to its simple system of equations.

IV. SELF-CONSISTENT PERTURBATION THEORY

In this section we perform the self-consistent perturbation calculations for the electric current. Instead of the standard perturbation calculation in Eq. (31), we take a self-consistent approach by dressing the bare Green's functions in the calculation of the self-energy, i.e.,

$$\Sigma^{\alpha}(t,t') = U^2 n_f(1-n_f)\frac{1}{N}\sum_{\mathbf{k}} G^{\alpha}(\mathbf{k}|t,t'). \tag{46}$$

In this approximation only the Green's functions of the conduction electrons are dressed. The Green's functions of the localized electrons are kept local; thus their contributions to the self-energy of the conduction electrons are just $n_f(1-n_f)$. We solve Kadanoff-Baym-Wagner equations (12)–(16) with the self-energy determined by Eq. (46). In order to solve these equations, we adopt the discretization method which was employed by Freericks *et al.*[20,27] in solving the NED-MFT equations. We discretize the time variables with step Δt for real time t and $\Delta\tau$ for imaginary time τ. As a result the real time domain is divided into L points, and the imaginary time domain β is divided into M points. Thus, any function of two time variables $A(\bar{t},\bar{t}')$ becomes a matrix $A_{ij}=A(\bar{t}_i,\bar{t}_j)$, where $\bar{t}_i=\bar{t}$ and $\bar{t}_j=\bar{t}'$. Integration over time can be approximated by the rectangular integration rule

$$\int d\bar{t}_1 A(\bar{t},\bar{t}_1)B(\bar{t}_1,\bar{t}') = \Delta\bar{t}\sum_l A(\bar{t}_i,\bar{t}_l)B(\bar{t}_l,\bar{t}_j),$$

where $\Delta\bar{t}=\Delta t$ for real time integration and $\Delta\bar{t}=-i\Delta\tau$ for imaginary time integration. Thus the time integration becomes a matrix multiplication. The inverse of the continuous matrix function

$$\int d\bar{t}_1 A(\bar{t},\bar{t}_1)A^{-1}(\bar{t}_1,\bar{t}') = \delta(\bar{t}-\bar{t}')$$

in the discretization approach becomes

$$\Delta\bar{t}\sum_l A(\bar{t}_i,\bar{t}_l)A^{-1}(\bar{t}_l,\bar{t}_j) = \frac{\delta_{ij}}{\Delta\bar{t}}. \tag{47}$$

Thus, in the discretization approach the Kadanoff-Baym-Wagner equations become the matrix equations which can be solved numerically. The time discretization is a numerical approach which approximately solves the Kadanoff-Baym-Wagner equations. It becomes exact only for $\Delta\bar{t}\to 0$. Nevertheless, it was shown that the discretization approach is an efficient way to solve the nonequilibrium Green's function equations.[20,27] Note that Kadanoff-Baym-Wagner equations (12)–(16) differ from the contour-ordered Green's-function equation.[20] Numerically, here we have to solve the equations of matrices with sizes $L\times L$, $L\times M$, and $M\times M$, instead of matrices of size $(2L+M)\times(2L+M)$ in the contour-ordered Green's-function equation. It reduces the matrix size and computation time. However, here we have to solve five equations with additional matrix multiplications. The inverse bare Green's functions $\tilde{G}_0^{\alpha}$ are calculated from Eqs. (6)–(10) with the inputs of the bare Green's functions in Eqs. (25)–(30). Within the discretization accuracy, these inverse bare Green's functions are calculated exactly. They satisfy the boundary conditions. For instance, the Matsubara Green's function has the antiperiodic property in the time variable, or the Keldysh Green's function satisfies $G_0^K(t_0,t_0)=2G_0^M(0,0^+)-i$. In the contour-ordered Green's-function approach, the inverse bare Green's function contains a time differential operator and it is also approximately discretized. In the present approach the inverse bare retarded and advanced Green's functions are numerically calculated from their bare functions by the discretization inverse relation in Eq. (47). The inverse Matsubara Green's function in the discretization form can be analytically obtained,

$$\tilde{G}_0^M(\mathbf{k}) = -\frac{i}{\Delta\tau^2}\begin{pmatrix} 1 & 0 & 0 & \cdots & & e^{-\varepsilon(\mathbf{k})\Delta\tau} \\ -e^{-\varepsilon(\mathbf{k})\Delta\tau} & 1 & 0 & \cdots & & 0 \\ 0 & -e^{-\varepsilon(\mathbf{k})\Delta\tau} & 1 & 0 & & \\ \vdots & \vdots & \vdots & & & \vdots \\ 0 & \cdots & \cdots & \cdots & -e^{-\varepsilon(\mathbf{k})\Delta\tau} & 1 \end{pmatrix}. \tag{48}$$

Here we have taken into account that $\mu_0=0$ at half filling. This inverse bare Matsubara Green's function corresponds to the bare Matsubara Green's function with fixed diagonal elements $G_0^M(\tau,\tau)=-i[1-f(\varepsilon(\mathbf{k}))]$. It is suitable for calculating the left time mixing Green's function because of the boundary condition $G_0^{\rceil}(\tau,t_0)=G_0^M(\tau,0)$ for $\tau\geq 0$. The right time mixing Green's function has the boundary condition $G_0^{\lceil}(t_0,\tau')=G_0^M(0,\tau')$ for $\tau'\geq 0$; the Matsubara Green's function suitable for its calculations has the diagonal elements $G_0^M(\tau,\tau)=if(\varepsilon(\mathbf{k}))$. The corresponding inverse bare Matsubara Green's function has the matrix form

$$\tilde{G}_0^M(\mathbf{k}) = \frac{i}{\Delta\tau^2}\begin{pmatrix} 1 & -e^{\varepsilon(\mathbf{k})\Delta\tau} & 0 & \cdots & 0 \\ 0 & 1 & -e^{\varepsilon(\mathbf{k})\Delta\tau} & \cdots & 0 \\ 0 & 0 & 1 & & \vdots \\ \vdots & \vdots & \vdots & & -e^{\varepsilon(\mathbf{k})\Delta\tau} \\ e^{\varepsilon(\mathbf{k})\Delta\tau} & \cdots & \cdots & 0 & 1 \end{pmatrix}. \tag{49}$$

For definiteness we also use this Matsubara Green's function for calculating the Keldysh Green's function. The Green's functions $\tilde{G}_0^{\rceil\lceil}$ can be also analytically obtained. From Eqs. (6)–(10), for the bare Green's functions in Eqs. (25)–(30) one can show that

$$\tilde{G}_0^{\rceil}(t,\tau') = \delta(t-t_0)\delta(\tau'), \tag{50}$$

$$\tilde{G}_0^{\lceil}(\tau,t') = -\delta(\tau)\delta(t'-t_0), \tag{51}$$

$$\tilde{G}_0^{K}(t,t') = i\delta(t-t_0)\delta(t'-t_0). \tag{52}$$

In the Keldysh formalism, when the time mixing Green's functions are neglected, the Green's function $\tilde{G}_0^K$ is little changed. One can obtain

$$\tilde{G}_0^K(t,t') = -i[2f(\varepsilon(\mathbf{k}))-1]\delta(t-t_0)\delta(t'-t_0). \tag{53}$$

In order to solve Kadanoff-Baym-Wagner equations (12)–(16), first we solve Eqs. (12) and (13) for the retarded (advanced) and Matsubara Green's functions, and then we find the time mixing Green's functions from Eqs. (14) and (15). Finally, the Keldysh Green's function is calculated from Eq. (16). We use iterations to solve each equation. When the nonequilibrium Green's functions are obtained, we can compute the electric current by using Eq. (38). The momentum summation in Eq. (46) and (38) indeed is the integration with the double Gaussian density of states in Eq. (24); we use a Gaussian quadrature to calculate it. Typically, we use 51 points for the Gaussian quadrature. In Sec. V we will discuss this type of integrations in detail. The calculated current converges with Δt well. We can obtain reliable results at $\Delta t \to 0$ by using a Lagrange interpolation formula. Typically, we use a quadratic interpolation to obtain the current in the continuous limit. In Fig. 5 we plot the electric current obtained within the Kadanoff-Baym-Wagner self-consistent perturbation theory. For comparison we also plot the exact NEDMFT calculation result (see also Sec. V). Figure 5 shows that the self-consistent perturbation theory gives very good results for times smaller than $2/U$. In comparison with the truncated perturbation theory, the self-consistent perturbation theory gives reasonable results in a wide range of the time variable. The current obtained within the self-consistent perturbation theory also oscillates with time and is damped to zero value. Even for large electric fields (for instance, $E=1$), the time damping of the current is still observed in the self-consistent perturbation results similar to the exact solution. However, for larger electric fields (for instance, $E=2$), the self-consistent perturbation theory cannot reproduce the beat behavior of the current, as shown in the lower panel of Fig. 5. It shows that the self-consistent perturbation theory may produce artifacts, especially for nonequilibrium steady state. However, this happens only for very strong electric fields. We define the initial correlation contribution to the current as the difference between the currents calculated within the Kadanoff-Baym-Wagner and the Keldysh self-consistent perturbation theories. In contrast to the results of the truncated perturbation theory, the initial correlation part of the current is damped with time, and its amplitude is significantly smaller. We plot the initial correlation contribution to the current for various values of U and E in Fig. 6. It shows that the amplitude of the initial correlation part is not scaled with U^2. For the long-time limit, the initial correlation contribution to the current vanishes. In this case the Keldysh and the Kadanoff-Baym-Wagner formalisms give the same steady state. However, it may be an artifact, especially for very strong electric fields when the exact current exhibits the beat behavior. This also indicates that the self-consistent perturbation theory may not work well for very strong electric

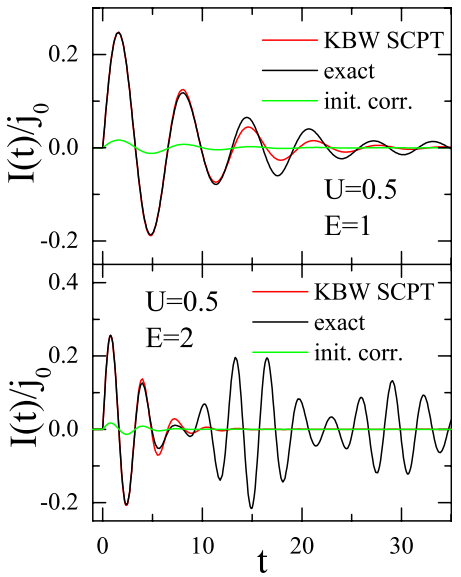

FIG. 5. (Color online) The time dependence of the electric current calculated within the KBW self-consistent perturbation theory (SCPT; red line). The exact NEDMFT calculation result and the initial correlation contribution to the current are presented as the black and green lines, respectively. The current was already scaled with a quadratic extrapolation (Δt=0.1, 0.065, and 0.05 and $\Delta\tau$ =0.1). The model parameters are U=0.5, t_0=−5, β=10, and E=1 (E=2) for the upper (lower) panel.

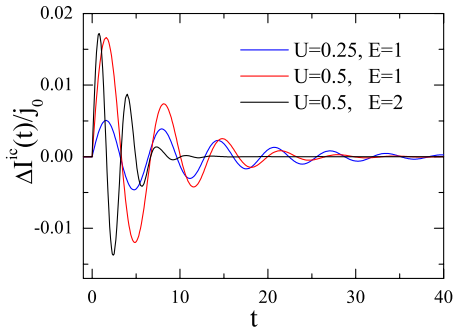

FIG. 6. (Color online) The time dependence of the initial correlation contribution to the current calculated within the Kadanoff-Baym-Wagner self-consistent perturbation theory for various U and E. The current was already scaled with a quadratic extrapolation ($\Delta t=0.1$, 0.065, and 0.05 and $\Delta\tau=0.1$). The other model parameters are $t_0=-5$ and $\beta=10$.

fields. Nevertheless, within the self-consistent perturbation theory, the Keldysh formalism qualitatively gives almost the same results as those of the Kadanoff-Baym-Wagner formalism. The initial correlations do not qualitatively change the perturbation results.

V. NONEQUILIBRIUM DYNAMICAL MEAN-FIELD THEORY

In this section we present the NEDMFT through the Kadanoff-Baym-Wagner representation. The NEDMFT was proposed by Freericks *et al.*[20] and it is based on the same idea as the DMFT in equilibrium. The NEDMFT has the same principal features as that of the equilibrium DMFT. It becomes exact in the infinite dimension limit. In infinite dimensions the self-energy is purely local in space. It can be determined by mapping the lattice problem onto an effective problem of a single site embedded in a self-consistent effective medium. The effective medium can be represented by a Green's function $\hat{\mathcal{G}}$ which is determined by the Dyson equation

$$\hat{G} = \hat{\mathcal{G}} + \hat{\mathcal{G}} \bullet \hat{\Sigma} \bullet \hat{G}, \tag{54}$$

where $\hat{G}=\Sigma_{\mathbf{k}}\hat{G}(\mathbf{k})/N$. From this equation we can find the components of the effective-medium Green's function in the Kadanoff-Baym-Wagner representation such as Eqs. (12)–(16). We obtain

$$\tilde{\mathcal{G}}^{R/A} = \tilde{G}^{R/A} + \Sigma^{R/A}, \tag{55}$$

$$\tilde{\mathcal{G}}^{M} = \tilde{G}^{M} + \Sigma^{M}, \tag{56}$$

$$\tilde{\mathcal{G}}^{\rceil} = \Sigma^{\rceil} - \tilde{G}^{R} \cdot G^{\rceil} \star \tilde{G}^{M}, \tag{57}$$

$$\tilde{\mathcal{G}}^{\lceil} = \Sigma^{\lceil} - \tilde{G}^{M} \star G^{\lceil} \cdot \tilde{G}^{A}, \tag{58}$$

$$\tilde{\mathcal{G}}^{K} = \Sigma^{K} - \tilde{G}^{R} \cdot G^{K} \cdot \tilde{G}^{A} + 2(\Sigma^{\rceil} - \tilde{\mathcal{G}}^{\rceil}) \star G^{\lceil} \cdot \tilde{G}^{A}, \tag{59}$$

where $\hat{\tilde{\mathcal{G}}}$ and $\hat{\tilde{G}}$ are the inverse matrices of $\hat{\mathcal{G}}$ and $\hat{G}$, respectively. Equations (55)–(59) are the Kadanoff-Baym-Wagner equations for determining the effective-medium Green's function $\hat{\tilde{\mathcal{G}}}$. Once the effective-medium Green's function $\hat{\tilde{\mathcal{G}}}$ is determined, we can compute the single-site Green's function. In the homogeneous phase we obtain[20]

$$\hat{G}_{\mathrm{imp}} = (1-n_f)\hat{Q}_0 + n_f\hat{Q}_1, \tag{60}$$

where n_f is the localized electron density and $\hat{Q}_l$ with $l=0,1$ satisfy the following equation:

$$[\hat{\tilde{\mathcal{G}}} + \Delta\mu - lU] \bullet \hat{Q}_l = \hat{1}. \tag{61}$$

Here $\Delta\mu=\mu-\mu_0$. One can find explicitly the components of $\hat{Q}_l$ by using the inverse equations [Eqs. (6)–(10)],

$$Q_l^{R/A} = [\tilde{\mathcal{G}}^{R/A} + \Delta\tilde{g}_l^{R/A}]^{-1}, \tag{62}$$

$$Q_l^{M} = [\tilde{\mathcal{G}}^{M} + \Delta\tilde{g}_l^{M}]^{-1}, \tag{63}$$

$$Q_l^{\rceil} = -Q_l^{R} \cdot \tilde{\mathcal{G}}^{\rceil} \star Q_l^{M}, \tag{64}$$

$$Q_l^{\lceil} = -Q_l^{M} \star \tilde{\mathcal{G}}^{\lceil} \cdot Q_l^{A}, \tag{65}$$

$$Q_l^{K} = -Q_l^{R} \cdot \tilde{\mathcal{G}}^{K} \cdot Q_l^{A} + 2Q_l^{R} \cdot \tilde{\mathcal{G}}^{\rceil} \star Q_l^{M} \star \tilde{\mathcal{G}}^{\lceil} \cdot Q_l^{A}, \tag{66}$$

where $\Delta\tilde{g}_l^{\alpha}=\tilde{g}^{\alpha}(\mu_0+\Delta\mu-lU)-\tilde{g}^{\alpha}(\mu_0)$, with $\alpha=R,A,M$, and $\tilde{g}^{\alpha}(x)$ is the inverse of the bare Green's function $g^{\alpha}(x)$ of a pure noninteracting single site with zero energy level and the chemical potential x. Note that in the numerical calculations, when we make the discretization of the time variable, the quantity $\Delta\mu-lU$ does not lie in the diagonal of the matrices of the inverse retarded (advanced) or Matsubara Green's functions. It lies in the first subdiagonal of the matrices like in Eqs. (48) and (49). In such way we can compute the single-site Green's function $\hat{G}_{\mathrm{imp}}$. However, it is applicable only to nonequilibrium FKM. For other models such as the Hubbard model one may adopt different techniques to solve the effective single-site problem.

The self-consistent condition requires that

$$\hat{G}_{\mathrm{imp}} = \hat{G}. \tag{67}$$

With this self-consistent condition, when the effective single-site problem is solved, we can again compute the self-energy from Kadanoff-Baym-Wagner equations (55)–(59). When the self-energy is obtained, the full lattice Green's functions are calculated from Kadanoff-Baym-Wagner equations (12)–(16). Thus we obtain a closed system of equations for the nonequilibrium Green's functions in the NEDMFT. Like in Sec. IV, first we solve the set of equations of the retarded (advanced) and Matsubara Green's functions. Then use the obtained Green's functions to solve the set of equations of the time mixing Green's functions. Finally, we compute the Keldysh Green's function from its set of equations. We use

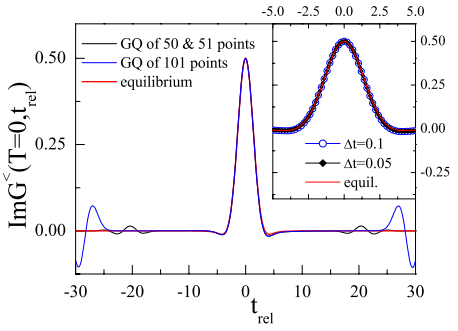

FIG. 7. (Color online) The imaginary part of the equilibrium lesser Green's function $\mathrm{Im}\, G^{<}(T=0,t_{\mathrm{rel}})$ calculated within the Kadanoff-Baym-Wagner NEDMFT by using two Gaussian quadratures (GQ) of 50 and 51 points (black line) and by one Gaussian quadrature of 101 points (blue line) ($\Delta t=0.1$, $\Delta\tau=0.1$, and $t_0=-15$) in comparison with the result calculated by solving the equilibrium DMFT equations in frequency (red line). The inset focuses on the imaginary part of the equilibrium lesser Green's function $G^{<}(T=0,t_{\mathrm{rel}})$ obtained by performing the two Gaussian quadratures of 50 and 51 points in a small range of t_{rel} for different Δt ($\Delta\tau=0.1$ and $t_0=-15$). The model parameters are $U=0.5$ and $\beta=10$.

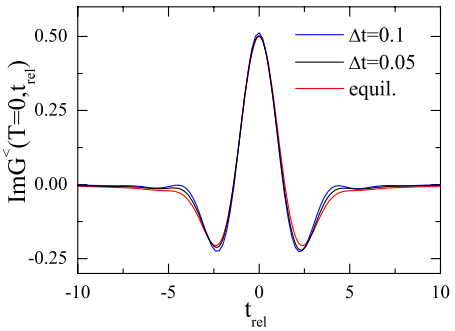

FIG. 8. (Color online) The imaginary part of the equilibrium lesser Green's function $\mathrm{Im}\, G^{<}(T=0,t_{\mathrm{rel}})$ calculated within the Kadanoff-Baym-Wagner NEDMFT for different Δt ($\Delta\tau=0.1$ and $t_0=-15$). The two Gaussian quadratures with 50 and 51 points are performed. The equilibrium DMFT calculation result is also presented (red line). The model parameters are $U=2$ and $\beta=10$.

iterations for finding each Green's function. Numerically, we employ the discretization method which was described in Sec. IV to solve the Kadanoff-Baym-Wagner NEDMFT equations. In equilibrium the FKM describes a metal-insulator transition for the homogeneous phase.[21–23] The Coulomb interaction is divided into two ranges. For weak interactions $(U<\sqrt{2})$ the system is metallic, and for strong ones $(U>\sqrt{2})$ the system is an insulator. We will study the two cases separately.

As a benchmark, we apply the Kadanoff-Baym-Wagner NEDMFT to the equilibrium FKM at half filling. The DMFT results of the FKM at equilibrium can be also obtained by solving the DMFT equations in frequency.[28] As noted in Sec. IV, the summation over momentum is replaced by integration with the double Gaussian density of states in Eq. (24); we use a Gaussian quadrature to perform the calculation. Freericks *et al.*[27] observed that averaging the results of two Gaussian quadratures with n and $n+1$ points works better than choosing $(2n+1)$ points for the quadrature. For the equilibrium case we adopt this trick. In Fig. 7 we plot the lesser Green's function $G^{<}(T,t_{\mathrm{rel}})=\Sigma_{\mathbf{k}}G^{<}(\mathbf{k}|T,t_{\mathrm{rel}})/N$ calculated within the Kadanoff-Baym-Wagner NEDMFT in comparison with the one obtained by solving the equilibrium DMFT equations in frequency. Here we have converted the results from the time variables t and t' to the Wigner average $T=(t+t')/2$ and relative $t_{\mathrm{rel}}=t-t'$ time variables. The NEDMFT calculations are performed with two Gaussian quadratures with 50 and 51 points. We also plot the NEDMFT result which is obtained by performing only one Gaussian quadrature with 101 points. The results plotted in Fig. 7 confirm the observation of Freericks *et al.* Indeed, for a range of small t_{rel} the lesser Green's function calculated within the NEDMFT matches perfectly the one obtained within the DMFT. However, for t_{rel} nearby the time cutoffs, the NEDMFT results exhibit spurious features of a nodal form due to the finite-size effects of the numerical procedures. These spurious features are greatly reduced by employing the trick of two Gaussian quadratures. However, as we will see later, the spurious features do not appear in the nonequilibrium case, where the electric field is finite. The lesser Green's function obtained within the NEDMFT fulfills the sum rule very well, as shown in the inset of Fig. 7. Indeed, $\mathrm{Im}\, G^{<}(T,t_{\mathrm{rel}}=0)\approx 0.5$ in the weak-interaction case. The sum rule of higher-order moments of the lesser Green's function is also fulfilled because the lesser Green's function matches perfectly the DMFT one nearby $t_{\mathrm{rel}}=0$. However, if one numerically calculates the sum rule of higher-order moments, a deviation from the exact value may appear due to numerical derivative calculations from discretized points.[29] The possible deviation of the sum rule of higher-order moment does not necessarily mean an inaccuracy of the Green's function. It relates to the finite value of Δt, which may be not small enough for performing numerical derivative calculations.

In Fig. 8 we plot the imaginary part of the equilibrium lesser Green's function calculated within the Kadanoff-Baym-Wagner NEDMFT and the equilibrium DMFT for $U=2$. This value of U corresponds to the insulator phase. It shows that for strong interactions the NEDMFT results match well the ones of the equilibrium DMFT for small t_{rel}. The spectral sum rule of the lesser Green's function is well fulfilled. Indeed, for $U=2$, $\mathrm{Im}\, G^{<}(T=0,t_{\mathrm{rel}}=0)$ is equal to 0.5123 for $\Delta t=0.1$ and is equal to 0.5021 for $\Delta t=0.05$. In comparison the exact value is 0.5. Around the minima in the curve of the imaginary part of the lesser Green's function, small deviations appear. The deviations can be reduced by decreasing Δt. For strong interactions the numerical results slightly deviate from the equilibrium values due to the finite discretization of the time variables. Nevertheless, the NEDMFT calculations for the equilibrium case for both weak and strong interactions show that the numerical techniques employed here are accurate and controllable.

In the nonequilibrium case, when the electric field is finite, we notice that the use of two Gaussian quadratures for the integration with the double Gaussian density of states gives almost the same result as the use of one Gaussian quadrature. In Fig. 9 we plot the imaginary part of the lesser Green's function calculated by using two Gaussian quadratures of 50 and 51 points in comparison with the one calcu-

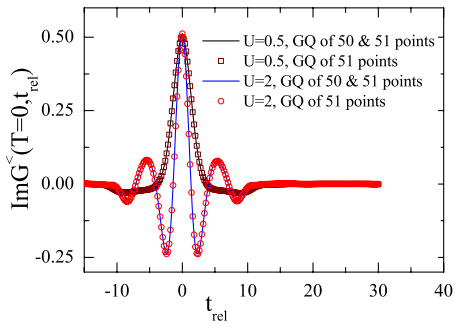

FIG. 9. (Color online) The imaginary part of the nonequilibrium lesser Green's function $\mathrm{Im}\, G^{<}(T=0,t_{\mathrm{rel}})$ calculated within the Kadanoff-Baym-Wagner NEDMFT by using two Gaussian quadratures of 50 and 51 points (solid lines), and by using one Gaussian quadrature of 51 points (symbols) for weak ($U=0.5$) and strong ($U=2$) interactions ($\Delta t=0.1$, $\Delta\tau=0.1$, $t_0=-15$, $\beta=10$, and $E=1$).

lated by using one Gaussian quadrature of 51 points for both weak and strong interactions. It shows that the results of both quadrature methods are almost identical. In contrast to the equilibrium case, in the nonequilibrium case there are no spurious features near the time cutoffs. We have also checked the results with more points for the Gaussian quadrature (in particular, with $n=101$), and with finer $\Delta\tau$ (in particular, with $\Delta\tau=0.05$). It turns out that the numerical results are mostly sensitive to the real time discretization. In the following for numerical calculations we use the single Gaussian quadrature with 51 points and make the integrations over the imaginary time with $\Delta\tau=0.1$ for $\beta=10$.

In Fig. 10 we present the lesser Green's function in the weak-interaction case for various real time discretizations Δt and a fixed t_0. It shows that the imaginary part of the lesser Green's function quickly converges with Δt. It also indicates that the spectral sum rule of the lesser Green's function is fulfilled well. In Table I we list the values of the spectral sum rule of the lesser Green's function for various values of Δt. In the Kadanoff-Baym-Wagner formalism, the spectral sum rule which is numerically calculated is fulfilled better than that in the formalism of the contour-ordered Green's function.[29] The spectral sum rule of the retarded and advanced Green's functions is fulfilled well too. The real part of the lesser Green's function converges with Δt is less quickly. However, it also converges well for small Δt. For weak interactions the numerical calculations solving the Kadanoff-Baym-Wagner NEDMFT equations work very well. For other physical quantities such as the electric current and the double occupation, their convergences with Δt are also good. In particular, we can obtain converged results at the limit $\Delta t\to 0$ by using a Lagrange interpolation formula.

TABLE I. The spectral sum rules of the nonequilibrium lesser Green's function at the average time $T=0$ calculated within the Kadanoff-Baym-Wagner NEDMFT for weak ($U=0.5$) and strong ($U=2$) interactions ($E=1$). Various values of Δt are used ($\Delta\tau=0.1$, $t_0=-15$, and $\beta=10$).

		$U=0.5$		
Δt	0.2	0.1	0.05	Exact
Sum rule	0.5007	0.5005	0.5004	0.5
		$U=2$		
Δt	0.1	0.05	0.025	exact
Sum rule	0.5123	0.5021	0.4983	0.5

In Fig. 11 we plot the lesser Green's function in the strong-interaction case for various real time discretizations Δt and a fixed t_0. The imaginary part of the lesser Green's function converges with Δt well. However, its spectral sum rule slightly deviates from the exact value, as presented in Table I. The real part of the lesser Green's function converges with Δt not so fast as in the weak-interaction case. In general, for strong interactions the extrapolations of the numerical results of the Kadanoff-Baym-Wagner NEDMFT in the limit $\Delta t\to 0$ require a greater effort. Often in order to obtain reliable data, we have to carry the numerical calculations with Δt smaller than the ones in the weak-interaction case.

One notices that the numerical results of the Kadanoff-Baym-Wagner NEDMFT are independent of the maximal time t_m when Δt and t_0 are fixed. We plot the electric current $I(t)$ obtained from the Kadanoff-Baym-Wagner NEDMFT

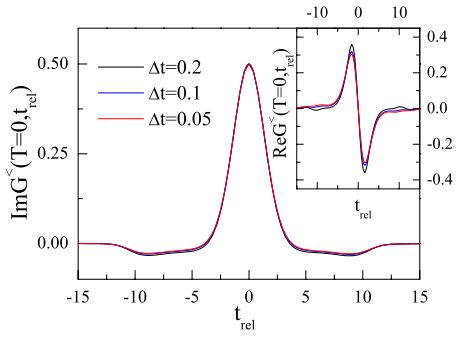

FIG. 10. (Color online) The imaginary part of the lesser Green's function $G^{<}(T=0,t_{\mathrm{rel}})$ calculated within the Kadanoff-Baym-Wagner NEDMFT in the weak-interaction case for various Δt. The inset plots the real part of the lesser Green's function. The model parameters are $U=0.5$, $E=1$, $\beta=10$, and $t_0=-15$. $n=51$ is used for the Gaussian quadrature and $\Delta\tau=0.1$.

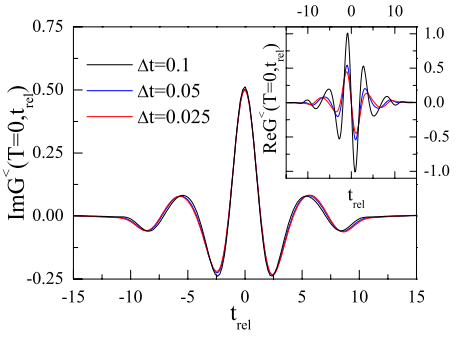

FIG. 11. (Color online) The imaginary part of the lesser Green's function $G^{<}(T=0,t_{\mathrm{rel}})$ calculated within the Kadanoff-Baym-Wagner NEDMFT in the strong-interaction case for various Δt. The inset plots the real part of the lesser Green's function. The model parameters are $U=2$, $E=1$, $\beta=10$, and $t_0=-15$. $n=51$ for the Gaussian quadrature and $\Delta\tau=0.1$.

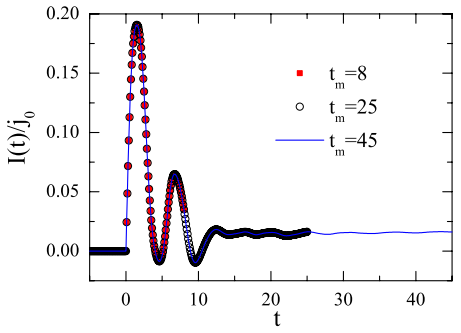

FIG. 12. (Color online) The time dependence of the electric current $I(t)/j_0$ calculated within the Kadanoff-Baym-Wagner NEDMFT for various time cutoffs t_m with fixed $\Delta=0.1$ and $t_0=-5$ ($U=2$, $E=1$, $\Delta\tau=0.1$, and $\beta=10$).

for various t_m in Fig. 12. For larger t_m the time window is larger and we can observe the behaviors of the system at a longer time. But for larger t_m the numerical calculations are also more expensive in time. We have to compromise the computation time and the need of the time window width.

In Fig. 13 we present the electric currents calculated within both the Kadanoff-Baym-Wagner and the Keldysh NEDMFTs in the weak-interaction case. In the Keldysh NEDMFT, the initial correlations are neglected. The contribution of the initial correlations to the current is defined as the difference between the currents calculated within the Kadanoff-Baym-Wagner and the Keldysh NEDMFTs. Certainly, the current has been previously calculated within the NEDMFT of the contour-ordered Green's function.[20] We find

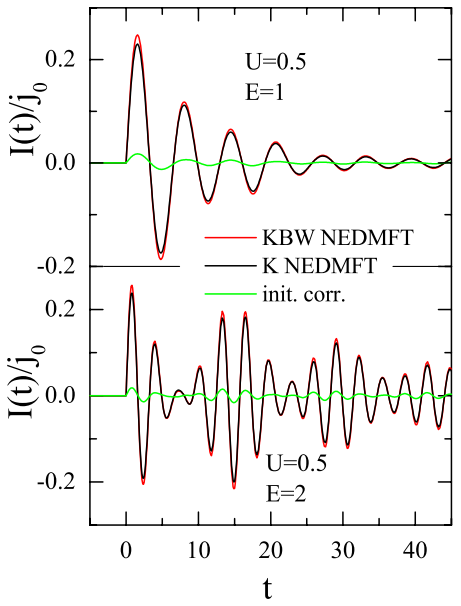

FIG. 13. (Color online) The time dependence of the electric current $I(t)/j_0$ calculated within the KBW NEDMFT (red line) in the weak-interaction case for different electric fields. For comparison, the result obtained from the K NEDMFT (black line) and the contribution of the initial correlations to the current (green line) are also plotted. The data are already scaled with a quadratic extrapolation ($\Delta t=0.1$, 0.065, and 0.05). The model parameters are $U=0.5$, $\beta=10$, and $\Delta\tau=0.1$. $E=1$ ($E=2$) for the upper (lower) panel.

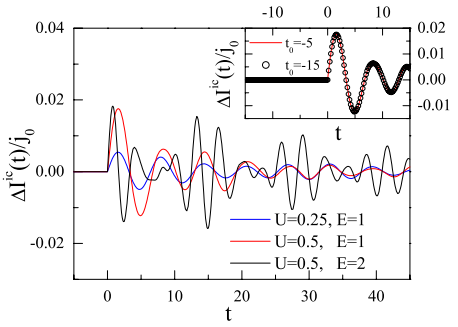

FIG. 14. (Color online) The time dependence of the contribution of the initial correlations to the electric current $\Delta I^{\rm ic}(t)/j_0$ for various E and U in the weak-interaction case. The results are already scaled by a quadratic extrapolation with $\Delta t=0.1$, 0.065, and 0.5 ($t_0=-5$, $\Delta\tau=0.1$, and $\beta=10$). The inset plots the scaled contribution of the initial correlations $\Delta I^{\rm ic}(t)/j_0$ for different initial times t_0 ($U=0.5$, $E=1$, $\Delta\tau=0.1$, and $\beta=10$).

that after extrapolating to $\Delta t\to 0$ the results of the Kadanoff-Baym-Wagner formalism agree well with the ones obtained within the contour-ordered Green's-function NEDMFT. This indicates the equivalence of the Kadanoff-Baym-Wagner and the contour-ordered Green's-function formalisms, as expected. However, the Kadanoff-Baym-Wagner formalism represents the contour-ordered Green's function in the matrix form, the elements of which are the physical Green's functions. It is also similar to the Keldysh formalism. The spectral sum rule obtained within the Kadanoff-Baym-Wagner NEDMFT is fulfilled very well. The electric current displays the Bloch oscillations, as observed by Freericks *et al.*[20] For small and large electric fields (for instance, $E=1$), the current is monotonously damped to zero value. However, when the electric field increases further (for instance, $E=2$), the current develops beats. As shown in Fig. 13, in the weak-interaction case the Keldysh and the Kadanoff-Baym-Wagner NEDMFTs qualitatively give the same current. The contribution of the initial correlations to the current also oscillates with time in the same way as that for the full current. When the current displays beats, the initial correlation contribution displays beats too, as shown in Figs. 13 and 14. In the weak-interaction case, the initial correlation contribution to the current is small in comparison with the full current. However, it never vanishes except for $t<0$ when the electric field is absent and the current vanishes too. In the inset of Fig. 14 we plot the initial correlation contribution to the current for different initial times t_0. It shows that the results are independent of the initial time if it is far enough from $t=0$. The initial correlation contribution seems to be finite even when the initial time is in the remote past. However, the initial correlations do not qualitatively change the current properties in the weak-interaction case.

We also calculate the double occupation $D(t)=\langle c^\dagger(t)c(t)f^\dagger(t)f(t)\rangle$, which can be computed through the lesser Green's function $Q_1^<(t,t)$ defined in Eq. (61) by using

$$D(t)=-in_f Q_1^<(t,t). \tag{68}$$

In Fig. 15 we plot the time dependence of the double occupation $D(t)$ calculated within the Kadanoff-Baym-Wagner

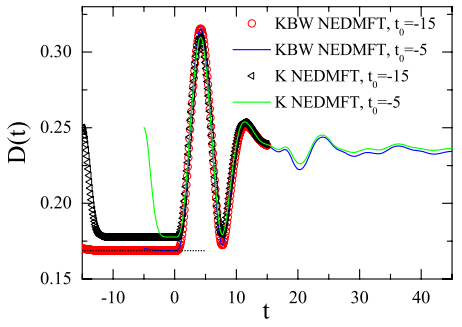

FIG. 15. (Color online) The time dependence of the double occupation $D(t)$ calculated within the KBW and the K NEDMFTs in the weak-interaction case for different initial times t_0. The results are already scaled by a quadratic extrapolation with $\Delta t=0.1$, 0.065, and 0.5. The dotted line is the double occupation at equilibrium ($E=0$). The model parameters are $U=0.5$, $E=1$, $\Delta\tau=0.1$, and $\beta=10$.

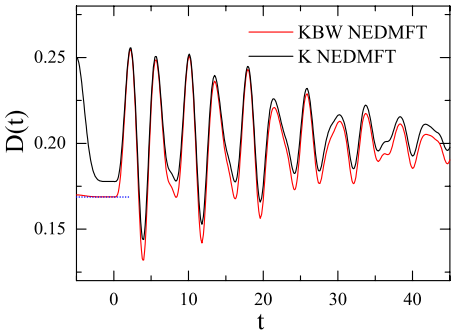

FIG. 16. (Color online) The time dependence of the double occupation $D(t)$ calculated within the KBW and the K NEDMFTs in the weak-interaction case for different initial times t_0. The results are already scaled by a quadratic extrapolation with $\Delta t=0.1$, 0.065, and 0.5. The dotted line is the double occupation at equilibrium ($E=0$). The model parameters are $U=0.5$, $E=2$, $\Delta\tau=0.1$, and $\beta=10$.

and the Keldysh NEDMFTs in the weak-interaction case. Before the electric field is turned on ($t<0$), the double occupation calculated within the Kadanoff-Baym-Wagner NEDMFT is constant and in good agreement with the equilibrium value obtained by solving the DMFT equations in frequency. However, the Keldysh NEDMFT results are quite different. Within the Keldysh NEDMFT, the double occupation starts from its noninteraction value at half filling ($D_0=0.25$), and then decreases to a steady value. This steady value is a little larger than the equilibrium value. At the initial time t_0, the Keldysh formalism starts with a noninteracting system and electron correlations are absent. The results show that before the electric field is turned on, the Keldysh formalism cannot restore the full electron correlations of the system. The full electron correlations are essentially elaborated from the initial correlations which come from the dynamics of the system in the imaginary time branch of the Kadanoff-Baym contour. The neglect of the initial correlations also means the lack of the electron correlations even when the system is still in equilibrium. In Fig. 15 we also plot the double occupation for different initial times t_0. It shows that even when the initial time approaches the remote past, the lack of electron correlations still occurs in the Keldysh formalism. Only in the Kadanoff-Baym formalism when the initial correlations are taken into account, full electron correlations are obtained. After the electric field is turned on ($t>0$) for weak and strong electric fields (for instance, $E=1$), the double occupation first oscillates strongly, and then is damped into less regular oscillations. However, when the electric field increases further (for instance, $E=2$), the double occupation regularly oscillates even for a long time, as shown in Fig. 16. This behavior is reminiscent of the beats of the electric current. In the weak-interaction case the difference between the double occupations calculated within the Kadanoff-Baym-Wagner and the Keldysh formalisms is small in relation to their values. After the turning on of the electric field, the difference becomes smaller. In the weak-interaction case the Keldysh formalism qualitatively describes the behavior of the double occupation.

In equilibrium when the interaction $U>\sqrt{2}$, the density of states opens a gap at the Fermi energy, and the system is an insulator. It distinguishes between the weak- and the strong-interaction cases. In general, in the strong-interaction case the numerical calculations slowly converge with Δt. Usually, we have to use more small values of Δt in order to get reliable results. In Fig. 17 we plot the electric current in the strong-interaction case. In contrast to the weak-interaction case, the current does not display the regular Bloch oscillations. The current oscillations are rather irregular and quenched. However, the current calculated within the Keldysh NEDMFT still exhibits the regular Bloch oscillations. This shows that the initial correlations are important in the strong-interaction case. They are a main factor for quenching the current oscillations. The contribution of the initial correlations to the current is not small as in the weak-interaction case. It is on the order of the current. In the inset of Fig. 17 we also plot the initial correlation contribution to the current for different initial times t_0. It shows that the contribution remains the same as the initial time approaches the remote past. Thus, in the strong-interaction case, the initial correlations become significant and dominate the overall properties of the current. The neglect of the initial correla-

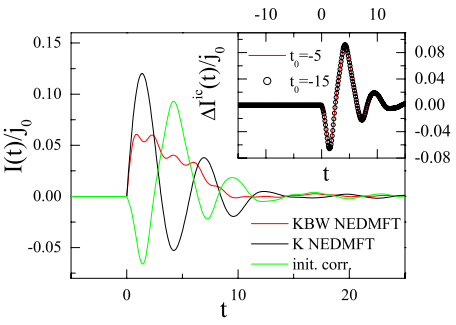

FIG. 17. (Color online) The time dependence of the electric current $I(t)/j_0$ calculated within the KBW and the K NEDMFTs for strong interaction, $U=2$ and $E=1$. The contribution of the initial correlations is also plotted. The inset plots the initial correlation contribution for different initial times t_0. The results are already scaled by a cubic extrapolation with $\Delta t=0.05$, 0.035, 0.025, and 0.02 ($\Delta\tau=0.1$ and $\beta=10$).

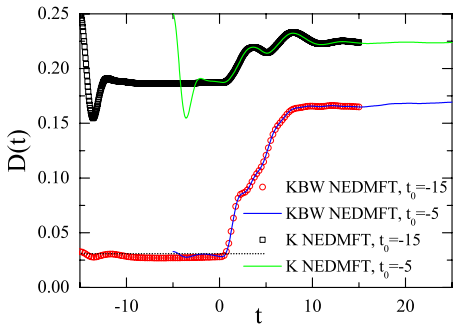

FIG. 18. (Color online) The time dependence of the double occupation $D(t)$ calculated within the KBW and the K NEDMFTs in the strong-interaction case for different initial times t_0. The results are already scaled by a cubic extrapolation with $\Delta t=0.05$, 0.035, 0.025, and 0.02. The dotted line is the double occupation at equilibrium ($E=0$). The model parameters are $U=2$, $E=1$, $\Delta\tau=0.1$, and $\beta=10$.

tions may cause artifacts in the nonequilibrium properties of the current.

In Fig. 18 we plot the double occupation in the strong-interaction case. Before the turning on of the electric field, the time dependence of the double occupation within both the Kadanoff-Baym-Wagner and the Keldysh NEDMFTs is similar to that in the weak-interaction case. Within the Kadanoff-Baym-Wagner formalism, the double occupation is constant for $t<0$. The constant value is in good agreement with the equilibrium value, although there are very little deviations due to the finite-size effects in the numerical calculations. The double occupation calculated within the Keldysh formalism first starts with the noninteraction value $D_0=0.25$ at the initial time t_0, and then relaxes to a steady value. Like in the weak-interaction case, the steady value is not the equilibrium value. It again indicates that the Keldysh formalism loses some part of electron correlations. In the strong-interaction case this lack of electron correlations becomes significant. As a consequence, after the turning on of the electric field, the lack of electron correlations also remains significant. Due to the quenching of the Bloch oscillations in the strong-interaction case, the double occupation reaches a steady value at a long time. The steady values obtained within the Kadanoff-Baym-Wagner and the Keldysh formalisms are quite different. They indicate the important contribution of the initial correlations. As shown in Fig. 18 the results do not change when the initial time is in the remote past. For strong interactions the Keldysh formalism loses a significant part of electron correlations both before and after the turning on of the electric field. It cannot correctly describe the nonequilibrium properties.

VI. CONCLUSIONS

In this paper we present the Kadanoff-Baym-Wagner formalism for nonequilibrium systems. The formalism is based on the Wagner representation of the contour-ordered Green's function. Within the Kadanoff-Baym-Wagner formalism, the Green's functions satisfy the proper boundary conditions. The initial correlations essentially distinguish between the Kadanoff-Baym-Wagner and the Keldysh formalisms. We derive the system of equations for nonequilibrium Green's functions, and solve it within the truncated and self-consistent perturbation theories as well as within the NEDMFT. As a benchmark, we examine the equilibrium FKM by the Kadanoff-Baym-Wagner NEDMFT. The results show good agreement between the Kadanoff-Baym-Wagner NEDMFT in equilibrium and the equilibrium DMFT. In the nonequilibrium case the Green's functions obtained within the Kadanoff-Baym-Wagner NEDMFT satisfy the spectral sum rule well. The derived Kadanoff-Baym-Wagner equations for nonequilibrium Green's functions are an alternative useful method for studying nonequilibrium systems.

In this paper we also emphasize the initial correlations. Within the perturbation theory the initial correlations are always finite even when the initial time goes to the remote past. The electric current calculated within the truncated perturbation theory shows that the Kadanoff-Baym-Wagner formalism overestimates the current, whereas the Keldysh formalism underestimates it. However, the Kadanoff-Baym-Wagner perturbation theory shows better agreement with the exact solution. For a long time the truncated perturbation theory fails to describe the physical properties. The self-consistent perturbation theory gives better results than those of the truncated perturbation theory. The time domain in which the self-consistent perturbation theory gives reasonable results is wider than the one in the truncated perturbation theory. However, the self-consistent perturbation theory cannot reproduce the beat behaviors of the current for very strong electric fields. Within the perturbation theories, the initial correlations do not qualitatively change the perturbation results. Since the Kadanoff-Baym-Wagner and the Keldysh perturbation theory results are close, the use of the Keldysh approach is more convenient since its equations are simpler. In the infinite dimension limit, the NEDMFT gives the exact solution. By examining the NEDMFT within both the Kadanoff-Baym-Wagner and the Keldysh formalisms, one can figure out the role of the initial correlations. For weak interactions the initial correlations give only small contributions to the physical quantities such as the electric current or the double occupation. However, they remain finite for the long-time limit. The initial correlations are also important even before the electric field is turned on when the system is still in equilibrium. Without the initial correlations the system cannot restore the full electron correlations. For strong interactions the initial correlations become significant and dominate the physical properties. Without taking into account the initial correlations, the Keldysh formalism can qualitatively describe the nonequilibrium properties of the system only for weak interactions. For strong interactions it fails to count full electron correlations. The neglect of the initial correlations may cause artifacts in the nonequilibrium properties of the system.

ACKNOWLEDGMENTS

The author would like to thank the Asia Pacific Center for Theoretical Physics, where the main part of this work was done, for its hospitality. He also acknowledges useful discus-

sions with Han-Yon Choi and thanks J. K. Freericks and V. Turkowski for providing their numerical data. The author is grateful to the Max Planck Institute for the Physics of Complex Systems at Dresden, where the numerical calculations were performed, for sharing computer facilities. This work was supported by the Asia Pacific Center for Theoretical Physics and in part by the Vietnam National Program on Basic Research.

[1] D. Goldhaber-Gordon, H. Shtrikman, D. Mahalu, D. Abusch-Magder, U. Meirav, and M. A. Kastner, Nature (London) **391**, 156 (1998).
[2] S. M. Cronenwett, T. H. Oosterkamp, and L. P. Kouwenhoven, Science **281**, 540 (1998).
[3] F. Simmel, R. H. Blick, J. P. Kotthaus, W. Wegscheider, and M. Bichler, Phys. Rev. Lett. **83**, 804 (1999).
[4] T. Ogasawara, M. Ashida, N. Motoyama, H. Eisaki, S. Uchida, Y. Tokura, H. Ghosh, A. Shukla, S. Mazumdar, and M. Kuwata-Gonokami, Phys. Rev. Lett. **85**, 2204 (2000).
[5] Y. Taguchi, T. Matsumoto, and Y. Tokura, Phys. Rev. B **62**, 7015 (2000).
[6] M. Greiner, O. Mandel, T. W. Hansch, and I. Bloch, Nature (London) **419**, 51 (2002).
[7] T. Kinoshita, T. Wenger, and D. S. Weiss, Nature (London) **440**, 900 (2006).
[8] R. Kubo, J. Phys. Soc. Jpn. **12**, 570 (1957).
[9] J. Schwinger, J. Math. Phys. **2**, 407 (1961).
[10] L. P. Kadanoff and G. Baym, *Quantum Statistical Mechanics* (Benjamin, New York, 1962).
[11] L. V. Keldysh, Sov. Phys. JETP **20**, 1018 (1965).
[12] P. Danielewicz, Ann. Phys. (N.Y.) **152**, 239 (1984).
[13] J. Rammer and H. Smith, Rev. Mod. Phys. **58**, 323 (1986).
[14] G. D. Mahan, *Many-Particle Physics*, 3rd ed. (Plenum, New York, 2000).
[15] S. Fujita, J. Phys. Soc. Jpn. **26**, 505 (1969).
[16] A. G. Hall, J. Phys. A **8**, 214 (1975).
[17] M. Wagner, Phys. Rev. B **44**, 6104 (1991).
[18] W. Metzner and D. Vollhardt, Phys. Rev. Lett. **62**, 324 (1989).
[19] A. Georges, G. Kotliar, W. Krauth, and M. J. Rozenberg, Rev. Mod. Phys. **68**, 13 (1996).
[20] J. K. Freericks, V. M. Turkowski, and V. Zlatic, Phys. Rev. Lett. **97**, 266408 (2006).
[21] L. M. Falicov and J. C. Kimball, Phys. Rev. Lett. **22**, 997 (1969).
[22] T. Kennedy, Rev. Math. Phys. **6**, 901 (1994).
[23] J. Jedrzejewski and R. Lemanski, Acta Phys. Pol. B **32**, 3243 (2001).
[24] J. K. Freericks and V. Zlatic, Rev. Mod. Phys. **75**, 1333 (2003).
[25] G. Stefanucci and C. O. Almbladh, Phys. Rev. B **69**, 195318 (2004).
[26] V. Turkowski and J. K. Freericks, Phys. Rev. B **75**, 125110 (2007).
[27] J. K. Freericks, V. M. Turkowski, and V. Zlatic, Proceedings of the HPCMP Users Group Conference 2005, Nashville, TN, 28–30 June 2005, edited by D. E. Post (IEEE Computer Society, Los Alamitos, CA, 2005), pp. 25–43.
[28] U. Brandt and C. Mielsch, Z. Phys. B: Condens. Matter **75**, 365 (1989).
[29] V. M. Turkowski and J. K. Freericks, Phys. Rev. B **73**, 075108 (2006).